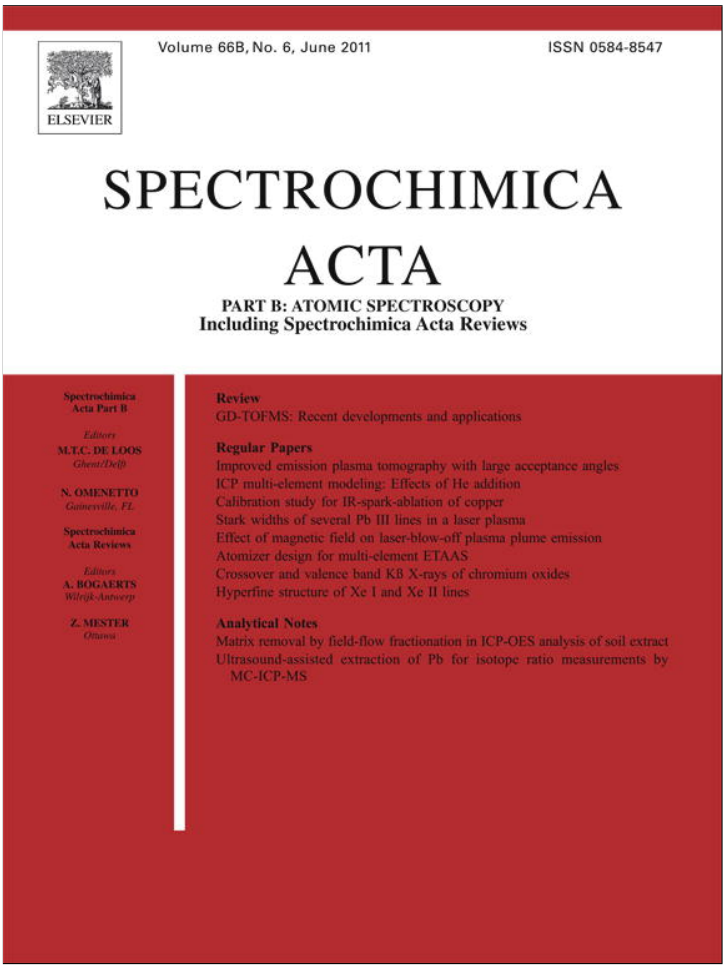

Spectrochimica Acta Part B 66 (2011) 470–475

Contents lists available at ScienceDirect

Spectrochimica Acta Part B

journal homepage: www.elsevier.com/locate/sab

Hyperfine structure of some near-infrared Xe I and Xe II lines

E. Pawelec [a,*], S. Mazouffre [b], N. Sadeghi [c]

[a] Opole University, Oleska 48, Opole, Poland
[b] ICARE, CNRS, 1C avenue de la Recherche Scientifique, 45071 Orléans, France
[c] LIPhy, Université Joseph Fourier Grenoble I & CNRS (UMR 5588), BP 87, 38402 Saint Martin d'Hères, France

ARTICLE INFO

Article history:
Received 12 November 2010
Accepted 31 May 2011
Available online 7 June 2011

Keywords:
Xenon
Saturation spectroscopy
Diode laser
Nuclear hyperfine structure

ABSTRACT

This work reports on the experimental determination of the hyperfine splitting of the Xe I lines at 828.01 nm and 834.68 nm and the Xe II line at 834.72 nm. Measurements were performed by means of Doppler-free saturation spectroscopy in a low-pressure radio-frequency discharge. The absolute wavelength of all hyperfine components is obtained by way of a high-precision wavemeter backed-up with the absorption spectrum of the NO_2 molecule. We provide an accurate estimate of hyperfine constants for the lower level of the Xe II transition at 834.72 nm. The two Xe I transition outcomes of our experimental study are compared with data available in the literature.

1. Background and goal

Spectra of rare gases are of interest in many areas of fundamental and applied physics. From a theoretical point of view, they give the possibility for verifying calculation of the properties of complicated quantum systems like heavy atoms which exhibit a rich electronic level pattern. The experimental investigation of nuclear effects on outer electrons for instance allows one to estimate difference in mean-square radii between isotopes, nuclear deformations, nuclear magnetic-dipole and electric-quadrupole interaction constants. Alternatively, when nuclear parameters are available, they provide information about electronic properties such as screening factors or electronic correlation effects. From a technical point of view, spectra of rare gases are needed to grasp the physics at work in various types of devices. For example, xenon (Xe) is currently used in gas-discharge lamps, plasma-display panels and as propellant in electric thrusters like gridded ion engines and Hall effect thrusters [1]. Understanding mechanisms that govern the plasma dynamics in these systems necessitates accurate measurements of physical parameters such as the particle temperature and velocity. In the case of nonequilibrium plasmas, one must directly access the atom and ion velocity distribution function. These quantities can often be determined by means of laser-aided diagnostics providing information about profiles of xenon atomic and ionic lines. However, due to the existence of numerous Xe isotopes, some with non-zero nuclear spin, analysis of measurements require precise knowledge of the isotopic shifts (IS) and hyperfine structures (HFS) of considered optical transitions.

Due to the quick development and widespread utilization of single-mode diode laser in the red and near-infrared spectral domain, Xe lines in the 800–910 nm wavelength range are at present often used for diagnosing xenon plasmas. The Xe I optical transitions $6s'[1/2]^\circ_2 \rightarrow 6p'[3/2]_2$ at 834.7 and $6s[3/2]^\circ_1 \rightarrow 6p[1/2]_0$ at 828.0 nm as well as the Xe II transition $5d\ ^4F_{7/2} \rightarrow 6p\ ^4D^\circ_{5/2}$ at 834.7 nm are readily probed by commercially-available diode lasers. The two transitions at 834.7 nm have proven to be especially useful for probing atoms and ions as they are two strong transitions very close to one another. Unfortunately, some of the isotopic shifts and hyperfine structure constants are unknown for both transitions. In this contribution, we present accurate measurements of line structure for the three aforementioned transitions of xenon by means of Doppler-free spectroscopy. This non-linear optical technique allows one to quantify the hyperfine splittings between all sublevels of the upper and lower states of the transition, which is the necessary step to extract hyperfine constants.

2. Previous studies

Isotope shifts and hyperfine structure in xenon have been measured in the past few years for many transitions with a large panel of experimental approaches. We here make a brief review of works dedicated to red and near-infrared Xe I and Xe II transitions.

Jackson and co-workers measured isotope shifts [2] and hyperfine splittings [3,4] in isotopically enriched samples for a wide variety of transitions in the visible and near-infrared spectral regions using interferometry with a 1 GHz resolution. They determined the hyperfine splittings of the lower level of Xe I 834.7 nm line. For the upper level, they were able to obtain the HFS constants only for the ^{129}Xe isotope. The resolution of their interferometer was indeed too

* Corresponding author.
E-mail address: ewap@uni.opole.pl (E. Pawelec).

0584-8547/$ – see front matter © 2011 Elsevier B.V. All rights reserved.
doi:10.1016/j.sab.2011.05.009

small for distinguishing the sublevels in the ^{131}Xe. A similar interferometric analysis of IS and HFS was performed by Fischer et al. [5]. A precise determination of the hyperfine splittings of the metastable Xe($^3P_2$) state was achieved by Faust and Dermott [6] by using the atomic beam nuclear magnetic resonance method.

High-resolution studies of optical IS and HFS have been facilitated by well consolidated Doppler-free laser spectroscopy techniques combined with the use of atomic beams. The IS and HFS constants of numerous short-lived xenon isotopes were investigated by collisional ionization laser spectroscopy at the ISOLDE facility at CERN [7]. Geisen et al. [8] investigated the $6s\ 1/2[1/2]_0 \rightarrow 8p1/2[1/2]_1$ transition at 626.5 nm and the $6s3/2[3/2]_2 \rightarrow 5d3/2[P]_3$ transition at 650.7 nm by means of Laser-Induced Fluorescence (LIF) spectroscopy on a beam of metastable Xe($^3P_2$) and Xe($^3P_0$) atoms.

The advent of semiconductor diode lasers allowed one to extend Doppler-free laser spectroscopy investigations in the near infrared spectral region. Saturated absorption spectroscopy on Xe atom was performed by Beverini et al. [9] and d'Amico et al. [10] with a diode laser emitting in the 820–830 nm range. In those works, four atomic transitions whose lower level is either metastable or resonant, namely the 820.26, 823.39, 826.88 and 828.24 nm lines, were interrogated in both an atomic beam and a low-temperature plasma source. One of the latest measurements based on saturated absorption technique was reported by Suzuki et al. [11]. Using a hollow cathode xenon discharge, authors studied nine infrared transitions in the 810–910 nm regions by two-frequency modulation of the laser beam. Among all results, they give parameters for the atomic line at 834.7 nm.

Finally, the IS and HFS of a few xenon ion lines were investigated in fast ion beam laser spectroscopy experiments. For instance, in the work by Broström et al. [12], three different transitions in isotopically enriched xenon samples were studied by LIF: the $5d\ ^4D_{7/2} \rightarrow 6p\ ^4P^\circ_{5/2}$ transition at 605.1 nm, the $5d\ ^4D_{7/2} \rightarrow 6p\ ^4D^\circ_{7/2}$ transition at 547.2 nm, and the $5d\ ^4D_{7/2} \rightarrow 6p\ ^4D^\circ_{5/2}$ transition at 553.1 nm. All these transitions have the $5d\ ^4D_{7/2}$ state in common. The 553.1 nm line involves the same upper state as the 834.7 nm transition of interest in this study.

3. Hyperfine structure

The list of studied transitions is shown in Table 1. The composition of the natural mixture of xenon isotopes is shown in Table 2. There are a multitude of even isotopes with different abundances. Those isotopes do not exhibit a hyperfine splitting as their nuclear spin is zero. The slight nucleus mass difference is, however, at the origin of an energy shift for all levels. The consequence is a slight difference in wavelength for a given transition of different isotopes, the so-called isotope shift. There are also two odd isotopes: ^{129}Xe and ^{131}Xe with a nuclear spin **I** of 1/2 and 3/2, respectively. Energy levels of those isotopes do exhibit a hyperfine splitting that is described by the total angular momentum quantum number $\mathbf{F}=\mathbf{I}+\mathbf{J}$, where **J** is the total angular momentum of electrons [13]. The energy shift of a sublevel is given by the sum of the magnetic dipole and the electric quadrupole contributions:

$$\Delta E = \Delta F_M + \Delta F_Q. \quad (1)$$

Table 1
Optical transitions investigated in this work.

Atom	Transition		J	λ in air [nm]
Xe I	$6s'[1/2]^\circ_1 \rightarrow 6p'[3/2]_2$	$1s_2 \rightarrow 2p_3$	1–2	834.6823
Xe I	$6s[3/2]^\circ_1 \rightarrow 6p[1/2]_0$	$1s_4 \rightarrow 2p_5$	1–0	828.0116
Xe II	$5d\ ^4F_{7/2} \rightarrow 6p\ ^4D^\circ_{5/2}$		7/2–5/2	834.7227
	$5d[4]_{7/2} \rightarrow 6p[3]^\circ_{5/2}$			

Table 2
Abundances of natural Xe isotopes (in %).

Isotope	124	126	128	129	130	131	132	134	136
Abundance	0.096	0.090	1.919	26.44	4.075	21.18	26.89	10.44	8.87

The two components read:

$$\Delta F_M = \frac{1}{2}A[F(F+1)-J(J+1)-I(I+1)] = \frac{1}{2}A\cdot R, \quad (2)$$

$$\Delta F_Q = \frac{1}{4}B\frac{\left[\frac{3}{2}R(R+1)-2J(J+1)I(I+1)\right]}{J(2J-1)I(2I-1)}, \quad (3)$$

where the numbers A and B are the magnetic dipole and electric quadrupole constants, respectively. From the theory of hyperfine interaction, the ratio between the magnetic dipole constants A of the ^{129}Xe and the ^{131}Xe isotopes scales as the ratio of their nuclear moments μ times the reciprocal of their respective nuclear spin. The ratio is equal to -0.2964. Note that $\mu_{129} = 0.7768\mu_B$ and $\mu_{131} = 0.6908\mu_B$, where μ_B is the Bohr magneton.

The selection rule for a hyperfine transition is $\Delta F = F - F' = [0,1]$. The $F = F' = 0$ transition is forbidden. Hyperfine splitting therefore gives 11 components for the Xe I line at 834.7 nm as can be seen in Fig. 1. Three components originate from ^{129}Xe and 8 from ^{131}Xe. The HF interaction also generates 5 components for the Xe I line at 828 nm and 12 components for the Xe II line at 834.7 nm. The intensity of any hyperfine component can be computed from Clebsch–Gordan coefficients [14]. Note that the relative intensity for each isotopic component can be calculated from the isotope abundance. In all the figures in this publication where the hyperfine component intensity is shown as a bar plot the relative intensities are calculated that way (they do not therefore include saturation).

4. Experimental arrangement

The hyperfine structure of a spectral line can be resolved when overcoming the limitation set by Doppler broadening. In this contribution, two non-linear absorption techniques based on selective saturation of individual atomic transitions were applied with the use of a tunable single-mode diode laser.

Preliminary results of those measurements without identification of the hyperfine components were published in [15].

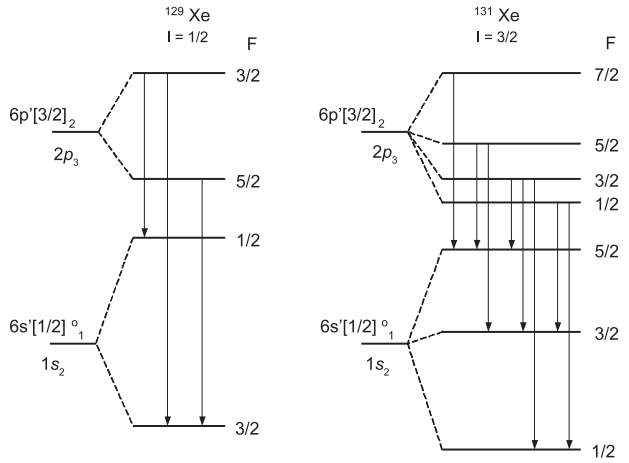

Fig. 1. Hyperfine components of the Xe I line at 834.68 nm. There are 11 allowed transitions and 6 HFS constants: $A^{129}_{2p_3}$, $A^{129}_{1s_2}$, $A^{131}_{2p_3}$, $B^{131}_{2p_3}$, $A^{131}_{1s_2}$, $B^{131}_{1s_2}$.

4.1. Plasma source

A low-pressure inductively coupled RF plasma discharge operating at 100 MHz is used as a source of excited atomic and ionic species [16]. The reactor consists of a helical antenna wrapped around a 10 cm in length and 1 cm in diameter quartz tube. No match-box unit is employed. Instead, a 50 Ω load is connected to one end of the antenna. The transmitted RF power is around 5 W, which maintains the gas temperature at the room temperature. The gas pressure is maintained at 0.03 Pa to ensure a high ionization degree of the injected xenon, which flows through the discharge cell at ~0.1 sccm to insure its purity. The low heavy particle and electron density in the plasma warrants pressure broadening and Stark broadening to be negligible in comparison with the broadening caused by the Doppler effect.

4.2. Saturated absorption

In the saturated absorption method, a pump beam with wave vector $+\vec{k}$ is used to create a "hole" in the velocity distribution function (VDF) of atoms, or ions, in long-lived metastable or resonant state [17]. When tuning the laser, the hole is solely detected at the line center by means of a weak counterpropagating probe beam that originates from the same laser, but of which the wave vector is $-\vec{k}$. The moving atoms perceive the two light beams as having different frequencies, due to the opposite Doppler shifts. However, at the line center, both pump and probe beams interact with the same atom, or ion, group experiencing a null velocity along the laser beam axis. The optical setup is depicted in Fig. 2. The holes in the absorption spectrum, the so-called Lamb-dips, exhibit a linewidth much smaller than the Doppler width, see the upper trace in Fig. 3. Modulating the pump laser beam intensity with a mechanical chopper and processing the probe laser beam signal with a lock-in amplifier allows the detection of the Lamb-dip with highly improved accuracy, as can be seen in Fig. 3. A calibrated high-precision (100 MHz) wavemeter backed up with the absorption spectrum of the NO_2 molecule enables determining the exact wavelength of each isotope and hyperfine component.

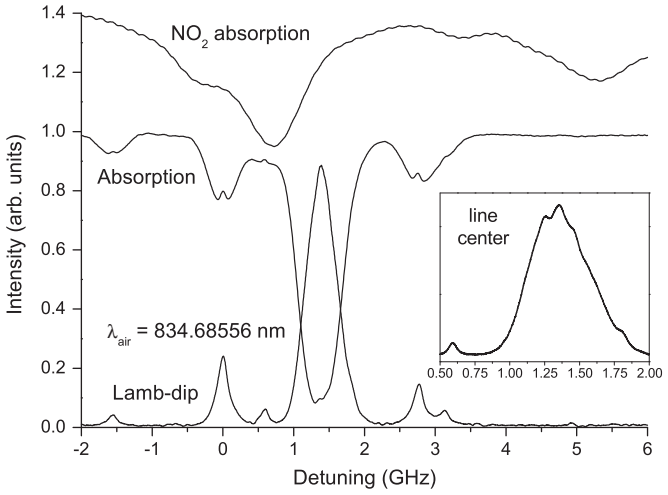

Fig. 3. Example of saturation spectroscopy outcomes for the atomic line at 834.68 nm. Also shown is the NO_2 absorption spectrum. A higher resolution profile of the main peak is shown in the inset.

4.3. Laser-Induced Fluorescence

Due to the low ionization degree in our plasma source, the amount of metastable ions is too weak for the optical transition to be studied by the absorption technique. One must then turn towards the Laser-Induced Fluorescence technique [18]. In our configuration, the saturation beam ($+\vec{k}$) and the much weaker (≈10% of the power) probe beam ($-\vec{k}$) are superimposed. The fluorescence light is detected at 90° with respect to the laser beam axis. The fluorescence

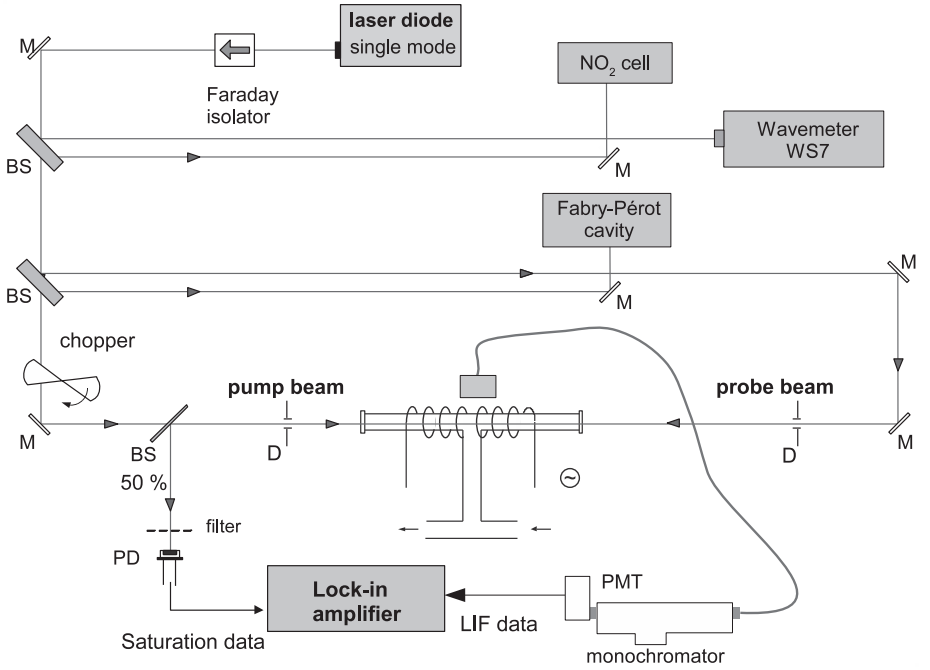

Fig. 2. Optical train. The first beamsplitter creates two secondary beams that are used for the NO_2 cell and the wavemeter. The second beamsplitter also yields two beams. One is directed to the Fabry–Pérot interferometer. The other serves as probe beam for saturation spectroscopy. The main beam serves as pump beam. Its intensity is modulated by way of a mechanical chopper. Two diaphragms warrant proper alignment of the beams. For absorption measurements, a third beamsplitter directs the probe beam to a photodiode. In the case of LIF measurements, the chopper is moved into the probe beam and the fluorescence radiation is collected at 90° and directed to the monochromator equipped with a photomultiplier tube.

wavelength is 473 nm and 542 nm when the laser is tuned on the 834.68 nm atom line and the 834.72 nm ion line, respectively. A schematic of the LIF bench is depicted in Fig. 2. When the probe beam intensity is modulated with a chopper and the fluorescence radiation is monitored at the modulation frequency, the observed lineshape exhibits Lamb-dips at line centers of each component. The resulting spectral profile can then be subtracted from the non-saturated one – acquired without the saturation beam – for obtaining the Lamb-dip profiles alone, as shown in Figs. 4 and 7.

4.4. Line broadening

The Doppler broadening of xenon lines at 300 K is of the order of 0.4 GHz. The sub-Doppler linewidth, which includes the natural width, the time-of-flight broadening and broadening due to the divergence angle and possible misalignment of the laser beams, can be estimated experimentally. A width of 50 MHz is obtained when the laser power is set to its minimum value, i.e. just before the Lamb dip vanishes. The Lamb dip width is in most cases larger than 50 MHz. This is due to the fact that the measured line components, especially the strongest, are strongly power-broadened during the saturation process.

5. Results and discussions

One of the specific feature of our measurements is the fact that the lineshapes are given with an absolute wavelength scale. This is achieved thanks to a combination of a Fabry–Pérot etalon, the NO_2 absorption spectrum and a calibrated high-precision wavemeter. The wavelength corresponding to the central peaks of the three investigated optical transitions agrees very well with the one available in the literature [19].

The 828 nm atomic line shown in Fig. 5 has a relatively simple structure. It was studied for comparison with other works, allowing therefore a kind of calibration procedure of our techniques. As can be seen in Table 3, the resulting HFS values are in good agreement with previously published data.

The main problem with the energy level structure of the 834.7 nm atomic line is the unresolved central peak that includes even isotope lines. Fig. 6 shows that the peaks within the central structure cannot be well separated and identified. In this figure, the spectral position of

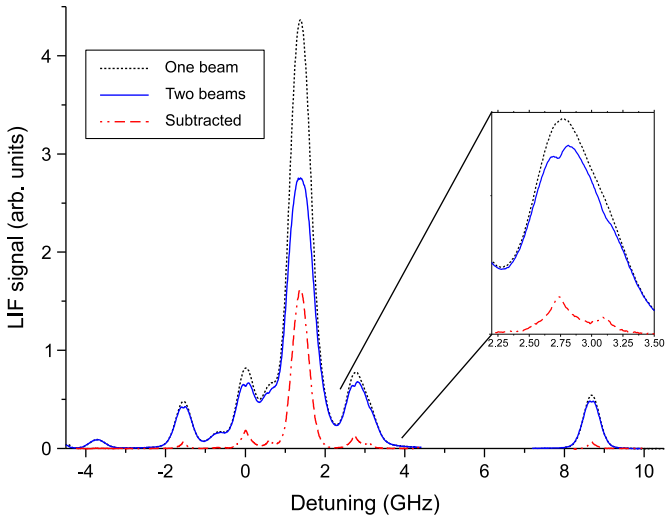

Fig. 4. Example of saturated LIF spectroscopy outcomes for the atomic line at 834.72 nm. One beam is a LIF signal with only the probe beam; two beams — LIF signal with both pump and probe beams; subtraction between the two signals yields the saturated-LIF signals. The inset shows an enlarged portion of the peak around 3 GHz.

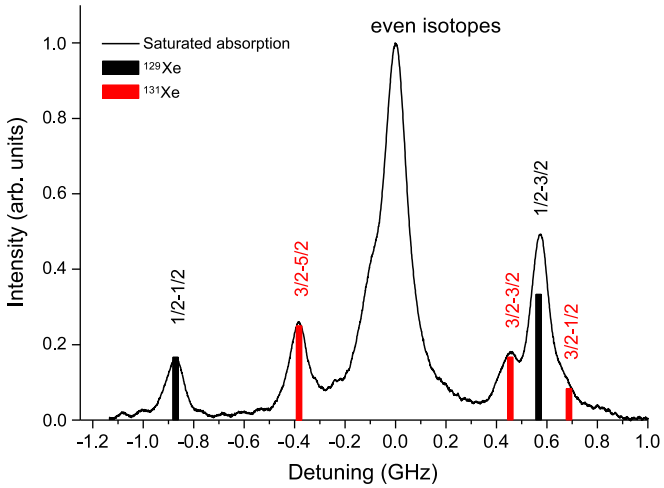

Fig. 5. Analysis of the 828.01 nm Xe atomic line recorded by saturated absorption method. Bars indicate the position and unsaturated amplitude of HF components.

the bars which correspond to the contribution of different even isotopes to the absorption profile is only indicative. As is seen in Fig. 3 of [10], their order must follow the isotopic mass and their amplitudes are proportional to the isotopic abundances. This remark holds also for Fig. 8. It is indeed difficult to decide which of the peaks belong to the even isotopes and which belong to the strongest components of hyperfine multiplet. The isotope shifts for even components should roughly vary linearly with the mass. The distribution of odd-isotope components is not well-defined which makes designation complicated. The values of the hyperfine splitting constants presented in Table 3 were all calculated from wavelength differences of the identified components of the measured hyperfine multiplets. Most of them are in good agreement with previously published values, but not all of them. Most visible differences are in the case of the A_{129} values for both levels of this transition. The main difficulty with the exact determination of those values is that they are in most cases calculated from only one frequency difference between the hyperfine components of the multiplet. Lines which belong to the ^{131}Xe isotope are numerous, so the possible error in the measured position of one component can be corrected using the rest of the set. The main source of error with older, interferometric measurements is probably the lower precision on the wavelengths of Doppler broadened lines. In the case of more recent Doppler-free measurements using diode lasers, see [11] and [10], error may arise from putting together individual

Table 3
Hyperfine splitting (in MHz) for levels investigated in this work.

Species	State	A129	A131	B131	Source
Xe I	$6s'\,[1/2]^\circ_1$ ($1s_2$)	−5805.5(6)	1712.4(6)	31.8(6)	[4]
		−5795(9)	1714.8(3)	24(6)	[5]
		−5808(2)	1709.3(0.7)	30.3(0.8)	[10]
		−5801.1(4.7)	1713.7(2.8)	24.5(8.5)	[11]
		−5788(5)	1706(6)	24(9)	This work
Xe I	$6s\,[3/2]^\circ_1$ ($1s_4$)	−963.8(3)	285.7(0.9)	86.9(18)	[4]
		−959.1(0.7)	284.3(0.6)	89.9(0.8)	[10]
		−960.3(4.7)	285.7(2)	92(2.7)	[11]
		−965(1)	287(2)	92(2)	This work
Xe I	$6p'\,[3/2]_2$ ($2p_3$)	−2891.5(6)			[4]
		−2894.6(4.7)	858.9(3.1)	−14.0(17)	[11]
		−2889(4)	829(4)	72(17)	This work
Xe II	$6p\,[3]^\circ_{5/2}$ ($6p\ ^4D^\circ_{5/2}$)	−1387(9)	409(2)	−117(10)	[12]
Xe II	$5d\,[4]_{7/2}$ ($5d\ ^4F_{7/2}$)	−955(5)	282(6)	−150(50)	This work

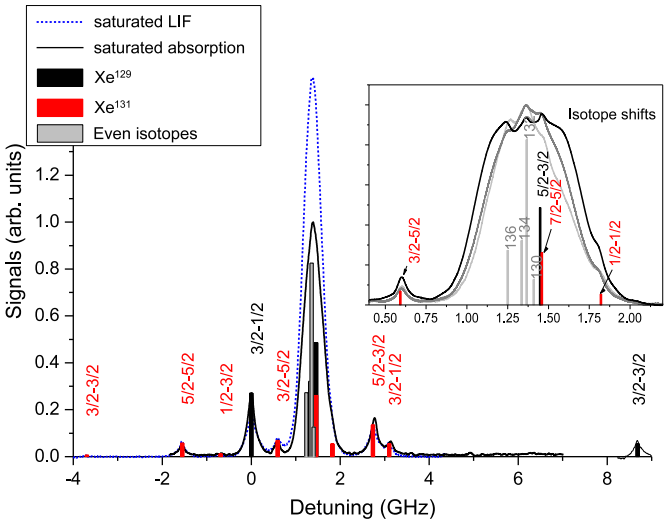

Fig. 6. Analysis of the 834.68 nm Xe atomic line by both saturated absorption and saturated LIF. Bars indicate the position and unsaturated amplitude of different components. The inset shows several more precise scans of the main peak with different saturation parameters.

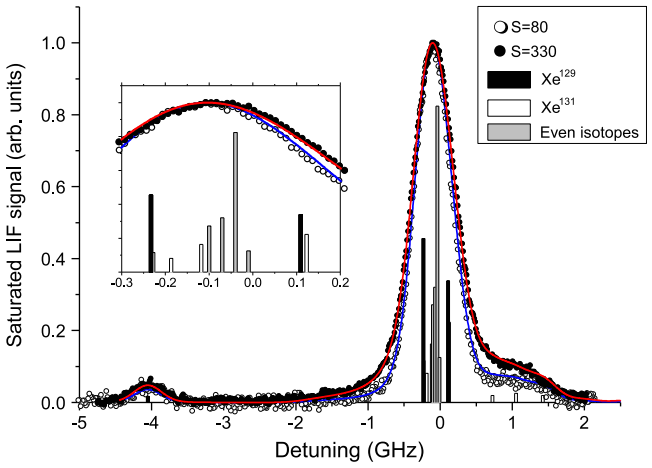

Fig. 8. Doppler-broadened profile of the 834.72 nm Xe ionic line recorded with two different values of the saturation parameter. Bars indicate the position and unsaturated amplitude of different components. The inset shows an enlarged portion of the main peak.

laser scans. A laser diode can hardly cover without mode hop the entire spectral range that stretches over 9 GHz for the Xe I 834.7 nm line. Several scans are then necessary with overlap regions. In our work, an accurate assembling of all spectra was possible as we employed very precise wavelength standards. It is therefore possible that previous measurements exhibit some systematic errors which were not included in the uncertainty calculation.

As can be seen in Fig. 8, the 834.7 nm Xe II line is very narrow. In a weak saturation Doppler-broadened regime, not much of its structure can be identified, as the main peak dominates. Even with slightly reduced width of the profile in the Doppler-free spectrum, this measurement does not improve significantly the resolution of the line components. Even in the low saturation limit the 50 MHz sub-Doppler linewidth is large enough to cause overlapping between components (see Fig. 7), and for the better signal/noise ratio one needs higher laser intensities. Doppler-free signals give therefore no more information than the ordinary LIF profiles, especially because when the saturation

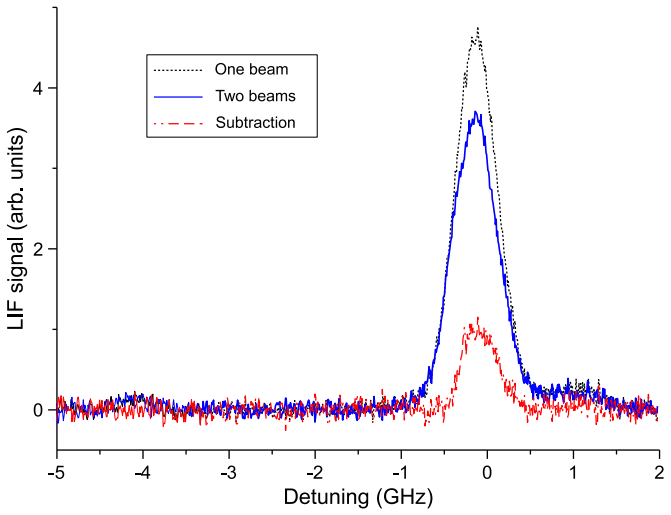

Fig. 7. Example of saturated LIF spectroscopy outcomes for the ionic line at 834.74 nm. One beam — LIF signal with only the probe beam; two beams — LIF signal with both pump and probe beams; subtraction between the two signals yields the saturated-LIF signal.

increases, the weak components in the Doppler-broadened profile become more visible. The analysis was therefore performed using the ordinary LIF signals. In order to assess the hyperfine structure, several measurement series were performed, each with a different saturation parameter, to allow a statistical analysis. Two spectra acquired with different laser powers are displayed in Fig. 8. HFS constants are finally determined from modeling of the Doppler-broadened measured line profiles. The model takes into account all pre-calculated components of the hyperfine structure. The Doppler and instrumental widths of each component are included by means of a Voigt profile. Saturation of the component is included in both the width and the amplitude of its Voigt profile [17]. Note that the HFS constants for the upper level of this transition were taken from [12], as the information contained in the profile is definitely not sufficient to obtain hyperfine coefficients for both levels.

6. Conclusion

In results reported by others [11] and presented in this article the xenon (atom and ion) lines at 834.7 nm are still not well resolved and the hyperfine and isotope shift data are still not completely reliable, though more and more data are present. These lines are rather easily observed from gas discharges, but the linewidth of signals measured in such sources even by applying sub-Doppler techniques is large enough to mask both the isotope shifts as some of the hyperfine structure. In the case of the ion line even the natural linewidth of the line is too large for the resolving of the main peak. Saturated LIF with a doubled beam modulation and lock-in detection at the sum frequency would be much more reliable, especially for ions, but the natural linewidth would still mask most of the structure, as some splittings are of definitely less than 40 MHz value.

The ideal situation for further analysis of these lines would be to investigate atoms and especially ions in enriched samples and much colder surroundings (if the lower level could be sufficiently populated), i. e. in atomic or ionic beams or traps, because even in isotopically enriched samples excited in a discharge there would still be difficult to determine precisely the peak wavelength. In the case of the ion 834.7 nm line, as the largest contribution to the sub-Doppler linewidth arises from the natural broadening due to the short lifetime of the level, thus more precise measurements would require very sophisticated traps. Still, the data shown here can be helpful in the analysis of signals measured for example in Hall thrusters, providing at least the hyperfine data if not isotope splittings for those two lines.

From both theoretical and applied-technical point of view, similar measurements for krypton could also be very interesting and both seriously enrich the knowledge of the atomic structure for noble gases and help the plasma diagnostics, as the hyperfine structure in krypton is less known than for xenon.

Acknowledgments

The authors greatly appreciate the technical assistance of P. Dom and N. Gouillon. This work was carried out with the support of the Région Centre.

References

[1] R.H. Frisbee, Advanced Space Propulsion for the 21st Century, J. Propul. Power 19 (2003) 1129–1154.
[2] D.A. Jackson, F.R.S. Coulombe, M.C. Coulombe, Isotope Shifts in the Arc Spectrum of Xenon, Proc. R. Soc. Lond. A 338 (1974) 277–298.
[3] D.A. Jackson, F.R.S. Coulombe, M.C. Coulombe, Hyperfine Structure in the Arc Spectrum of Xenon, Proc. R. Soc. Lond. A 327 (1972) 137–145.
[4] D.A. Jackson, F.R.S. Coulombe, M.C. Coulombe, Hyperfine Structure in the Arc Spectrum of Xenon. II, Proc. R. Soc. Lond. A 335 (1973) 127–140.
[5] W. Fischer, H. Huhnermann, G. Kromer, H.J. Schafer, Isotope Shifts in the Atomic Spectrum of Xenon and Nuclear Deformation Effects, Z. Phys. 270 (1974) 113–120.
[6] W.L. Faust, M.N. McDermott, Hyperfine Structure of the (5p)5(6s)3P2 State of 54Xe129 and 54Xe131, Phys. Rev. 123 (1961) 198–204.
[7] W. Borchers, E. Arnold, W. Neu, R. Neugart, K. Wendt, G. Ulm, Xenon isotopes far from stability studied by collisional ionization laser spectroscopy, Phys. Lett. B 216 (1989) 7–10.
[8] H. Geisen, T. Krumpelmann, D. Neuschafer, Ch. Ottinger, Hyperfine splitting measurements on the 6265 A and 6507 A lines of seven Xe isotopes by LIF on a beam of metastable Xe(3P0,2) atoms, Phys. Lett. A 130 (1988) 299–304.
[9] N. Beverini, G.L. Genovesi, F. Strumia, Xenon saturation spectroscopy by diode laser, Nuovo Cimento D 17 (1995) 515–522.
[10] G. D'Amico, G. Pesce, A. Sasso, Isotope-shift and hyperfine-constant measurements of near-infrared xenon transitions in glow discharges and on a metastable Xe(3P2) beam, Phys. Rev. A 60 (1999) 4409–4416.
[11] M. Suzuki, K. Katoh, N. Nishimiya, Saturated absorption spectroscopy of Xe using a GaAs semiconductor laser, Spectrochim. Acta Part A 58 (2002) 2519–2531.
[12] L. Broström, A. Kastberg, J. Lidberg, S. Mannervik, Hyperfine-structure measurements in Xe II, Phys. Rev. A 53 (1996) 109–112.
[13] G.K. Woodgate, Elementary Atomic Structure, Clarendon, Oxford, 1980.
[14] E.U. Condon, G.H. Shortley, The Theory of Atomic Spectra Cambridge, Cambridge University Press, 1935.
[15] S. Mazouffre, E. Pawelec, N. Tran Bich, N. Sadeghi, Doppler-Free Spectroscopy Measurements of Isotope Shifts and Hyperfine Components of Near-IR Xenon Lines, AIP proceedings of the International Conference Plasma 2005 comb. with 3rd GPPD and the 5th FPS, Melville, New York, 2006.
[16] D. Gawron, S. Mazouffre, N. Sadeghi, T. Gibert, A. Bouchoule, Time-resolved LIF study on xenon plasma decay after fast interruption: Applications to Hall effect thruster, Proceedings of the 6th Workshop on Frontiers in Low Temperature Plasma Diagnostics, Les Houches, France, 2005.
[17] W. Demtröder, Laser Spectroscopy, Springer-Verlag, Berlin Heidelberg, 2003.
[18] T. Nakano, N. Sadeghi, D.J. Trevor, R.A. Gottscho, R.W. Boswell, Metastable chlorine ion transport in a diverging field electron cyclotron resonance plasma, J. Appl. Phys. 72 (1992) 3384–3393.
[19] Yu Ralchenko, A.E. Kramida, J. Reader, NIST ASD Team, NIST Atomic Spectra Database (version 3.1.5), [Online] Available, National Institute of Standards and Technology, Gaithersburg, MD, 2008. http://physics.nist.gov/asd3 [2008, October 6].